JOURNAL OF IRON AND STEEL RESEARCH, INTERNATIONAL. 2014, 21(11): 1009-1015

Slag/metal Separation Process of Gas-reduced Oolitic High-phosphorus Iron Ore Fines

Hui-qing TANG, Long MA, Jun-wei WANG, Zhan-cheng GUO
(State Key Laboratory of Advanced Metallurgy, University of Science and Technology Beijing, Beijing 100083, China)

Abstract: Slag/metal separation process of the highly reduced oolitic high-phosphorus iron ore fines was investigated. Samples were prepared using the reduced ore fines (metallization rate: 88%) and powder additives of CaO and Na_2CO_3. Slag/metal separation behavior tests were conducted using a quenching method and the obtained metal parts were subjected to direct observation as well as microstructure examination with SEM and EDS; iron recovery and phosphorus distribution tests were conducted using a Si-Mo high temperature furnace and the obtained metal parts were examined by ICP-AES analysis and mass measurement. Thermodynamic calculation using coexistence theory of slag structure was also performed. Results show that temperature for slag/metal separation must be higher than 1823 K and a satisfying slag/metal separation of the highly reduced ore fines needs at least 4 min; phosphorus content of hot metal is mainly determined by thermodynamics; temperature of 1823—1873 K and Na_2CO_3 mixing ratio of about 3% are adequate for controlling phosphorus content to be less than 0.3 mass% in hot metal; temperature, time and Na_2CO_3 mixing ratio do not have significant effect on iron recovery, and iron recovery rate could be higher than 80% as long as a good slag/metal separation result is obtained.

Key words: oolitic high-phosphorus iron ore fine; slag/metal separation; iron recovery; phosphorus partition

A number of technical routes have been proposed on processing the oolitic high-phosphorus iron ore in China[1-4]. Gaseous reduction followed by melting separation to directly produce low-phosphorus hot metal, which was proposed by the authors of current study[5], is one of the feasible routes. Metallization rate of the fines could exceed 85% by applying microwave pretreatment to the ore fines in gaseous reduction stage[6]. Because of the high reduction degree of the fines, the subsequent step, slag/metal separation process, needs further study to maximize iron recovery rate and minimize phosphorus level in hot metal. Many factors could affect phosphorus partition ratio and iron recovery rate in slag/metal separation process. For example, additive CaO can significantly change phosphorus partition ratio in melting separation of the ore fines with a metallization of 65% in the previous tests of current authors[5].

In the present research, effects of temperature and time on the slag/metal separation were studied. Additionally, Na_2CO_3 as a new additive was introduced for its low cost and has been found effective for dephosphorization of molten pig iron and hot metal[7,8], therefore its effect on the slag/metal separation process was investigated as well.

1 Experimental

1.1 Sample preparation

The oolitic high-phosphorus iron ore was supplied by Wuhan Iron and Steel Company. Composition of the ore sample is listed in Table 1. The ore sample was crashed and ground to a size less than 1 mm.

The ore fines were reduced using an intensified

Table 1 Composition of oolitic high-phosphorus iron ore sample mass%

TFe	CaO	SiO_2	MgO	MnO	Al_2O_3	P
49.2	1.97	12.4	0.48	0.38	6.2	0.81

Foundation Item: Item Sponsored by National Natural Science Foundation of China (51144010); Research Funds from State Key Laboratory of Advanced Metallurgy USTB of China (416020020)
Biography: Hui-qing TANG, Doctor, Associate Professor; **E-mail**: hqtang@ustb.edu.cn; **Received Date**: January 13, 2013

gaseous reduction method as described in Ref. [5]. Average final metallization rate of the fines for this research was about 88%. Powder additives (chemically pure CaO and Na_2CO_3) were then well mixed with the reduced fines to prepare samples. Mixing ratio of CaO to the reduced fines satisfied that basicity (w_{CaO}/w_{SiO_2} in mass%) of the sample was 1.0 and mixing ratio of Na_2CO_3 varied for different purposes.

1.2 Slag/metal separation behavior trials

Quench method was adopted in these runs. Firstly, an Si-Mo high temperature furnace was heated to a predetermined temperature, and then highly pure argon at a flow rate of 200 mL/min was introduced into the chamber of the furnace. Sample with basicity of 1.0 and Na_2CO_3 mixing ratio of 2.0% was used. In each run, 5—7 g sample was put in an Al_2O_3 crucible (ϕ30 mm×45 mm) which was protected by a graphite crucible. It was then inserted quickly into the chamber and slag/metal separation test started. Melting time was calculated when the furnace temperature returned back. The sample was quenched after holding in the chamber for a given time. Thereafter its cross-section image was taken for examination of slag/metal separation result; its microstructure was examined by SEM and EDS.

1.3 Phosphorus distribution and iron recovery trials

After time and temperature for satisfying slag/metal separation were determined, experiments on phosphorus distribution and iron recovery were carried out. Samples with basicity of 1.0 and different Na_2CO_3 mixing ratios were used. In each run, 30—35 g sample was put in an Al_2O_3 crucible (ϕ45 mm×115 mm) which was also protected by a graphite crucible. It was then placed in the chamber of the Si-Mo furnace. The sample was heated up to the predetermined temperature at a heating rate of 10 K/min. After holding for the predetermined time, the sample was allowed to cool down to 773 K at 10 K/min and then to room temperature naturally. During the whole separation process, inert gas atmosphere was kept by highly pure argon flow of 200 mL/min in the chamber. The obtained metal part was weighed and iron recovery rate was estimated by Eq. (1).

$$\eta=\frac{m_{obt}}{m_{tot}}\times 100\% \quad (1)$$

where, η is iron recovery rate; m_{obt} is mass of the obtained metal part; and m_{tot} is total iron mass in the sample.

Phosphorus contents of the metal and the slag were measured using ICP-AES analysis.

2 Results and Discussion

2.1 Slag/metal separation behavior

2.1.1 *Effect of melting temperature*

Three temperature levels were examined. Fig. 1 shows cross-section images of the obtained metal parts and Fig. 2 shows their microstructures. From Fig. 1(a), it could be seen that, at 1773 K, shape of the metal part is near the melting crucible; slag particles in the metal are clearly visible and many pores and flaws spread on its cross-section. From Fig. 2(a), it could be seen that a distinct boundary exists between metal phase and slag phase as indicated by EDS results (Points 1 and 2). It is thus judged that the sample was only partially melted at 1773 K. At 1773 K, unmelted solid phase inhibits coalescence and growth of slag droplets and hot metal droplets; therefore, these droplets could move only in a short distance and slag/metal separation failed. From Figs. 1(b) and 1(c), it could be seen that the slag/metal separation is greatly improved when melting temperature is higher than 1823 K. Slag particles and flaws

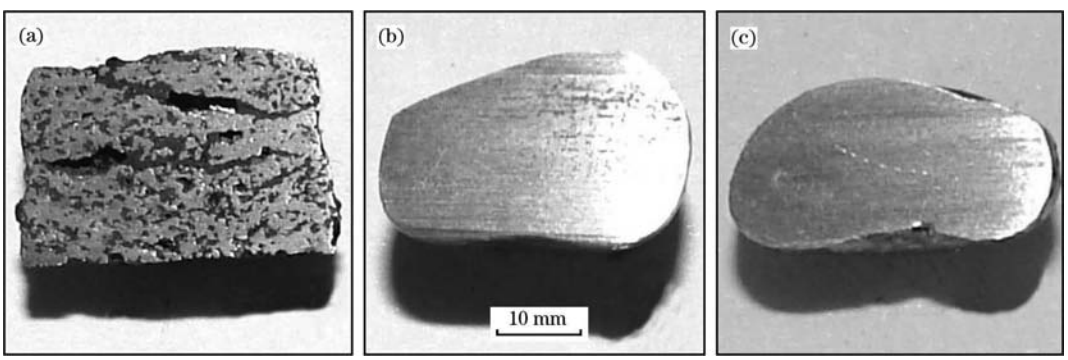

Melting time: 10 min; Na_2CO_3 mixing ratio: 2%.
(a) 1773 K; (b) 1823 K; (c) 1873 K.

Fig. 1 Cross-section images of the metal parts obtained at different melting temperatures

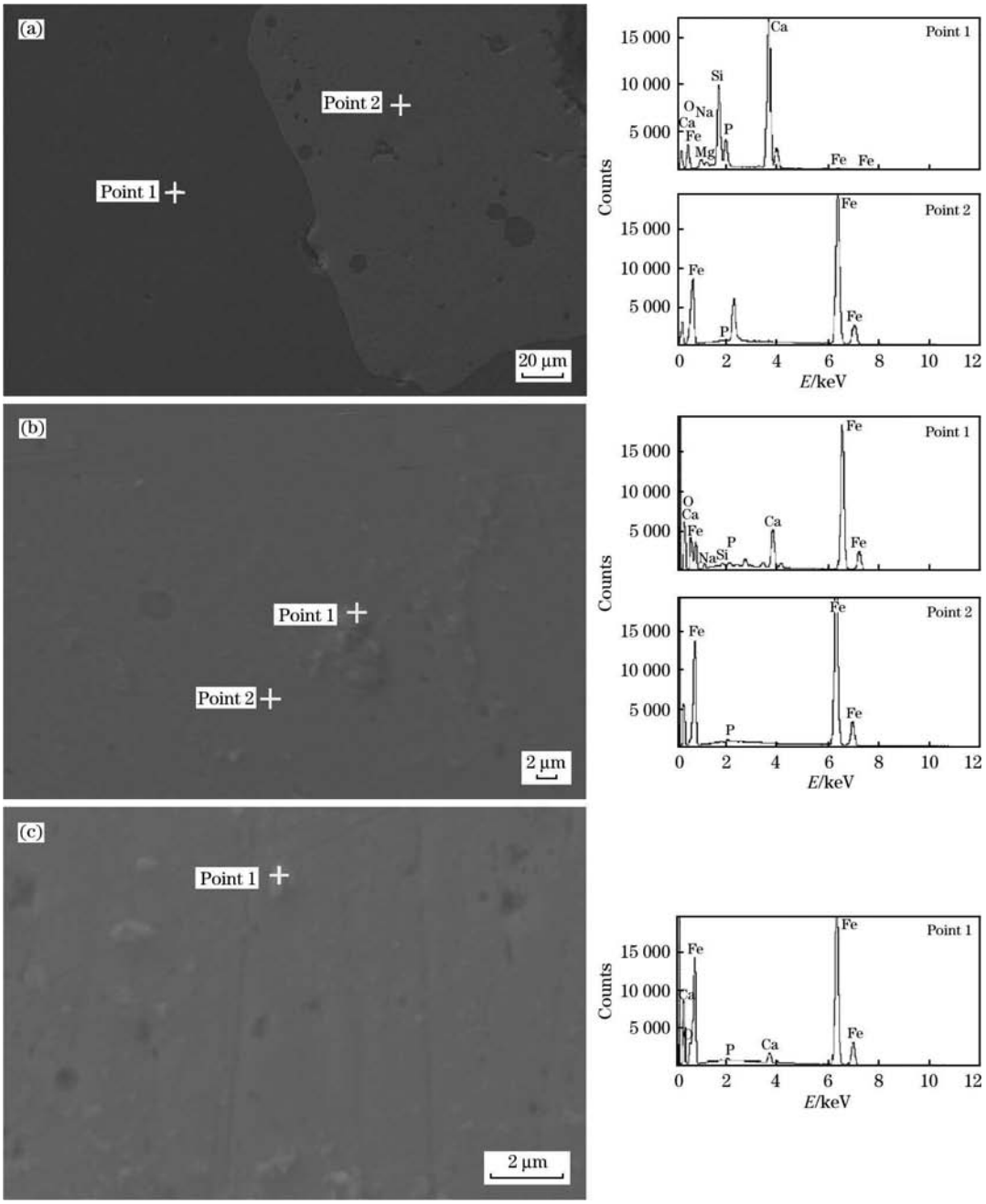

Melting time: 10 min; Na_2CO_3 mixing ratio: 2%.
(a) 1773 K; (b) 1823 K; (c) 1873 K.

Fig. 2 SEM images and EDS results of the metal parts obtained at different melting temperatures

could not be easily observed in metal, and both of the two metal parts have a near-sphere shape due to the surface tension of hot metal at high temperature; moreover, the two metal parts exhibit some metal properties. Comparing Fig. 1(c) to Fig. 1(b), the difference is that some slag lines could be found in the cross-section of the metal part obtained at 1823 K while they could not be found in the metal part obtained at 1873 K. As temperature is higher than 1823 K, reduced ore fines could be fully melted. Fluidity of hot metal and liquid slag thereby increases; therefore, hot metal droplets sink and liquid slag droplets float up in the crucible, coalescing and forming the final metal part and slag part respectively. Their microstructures are given in Figs. 2(b) and 2(c). EDS results (Point 1 in Fig. 2(b) and Point 1 in Fig. 2(c)) show the detected particles are slag inclusions and EDS result (Point 2 in Fig. 2(b))

show that the detected area is metallic iron. Figs. 2 (b) and 2(c) show that slag inclusions and pores are randomly distributed in metallic iron; however, in the metal part obtained at 1873 K, they are much smaller. Viscosity of hot metal decreases with the increase of temperature, so slag inclusion and gas bubble removal efficiencies are improved. Though increasing temperature favors improving slag/metal separation, it is considered that melting temperature above 1823 K could ensure a satisfying slag/metal separation.

2.1.2 Effect of melting time

Fig. 3 shows sequential cross-section images of the obtained metal parts at 1823 K and Fig. 4 shows their microstructures. From Figs. 3 and 4, it is assumed that the sample experienced the following four steps in the melting process. At melting time of 1 min, most of ore fines sintered together as their surfaces were melted, and the sample presented a shape nearly like the melting crucible (Fig. 3 (a)), however, oolitic structure in the ore fine remained unchanged in this stage (Fig. 4(a)). At melting time of 2 min, the sample underwent a volume shrinkage as amount of liquid phase increased in the sample and its porosity was then reduced, however amount of solid phase in this stage was still enough to support its initial shape (Fig. 3(b)); oolitic structure in the ore fine was destroyed, metallic iron tended to be in the outer area of the fine and slag concentrated in its core area (Fig. 4(b)). At melting time of 3 min,

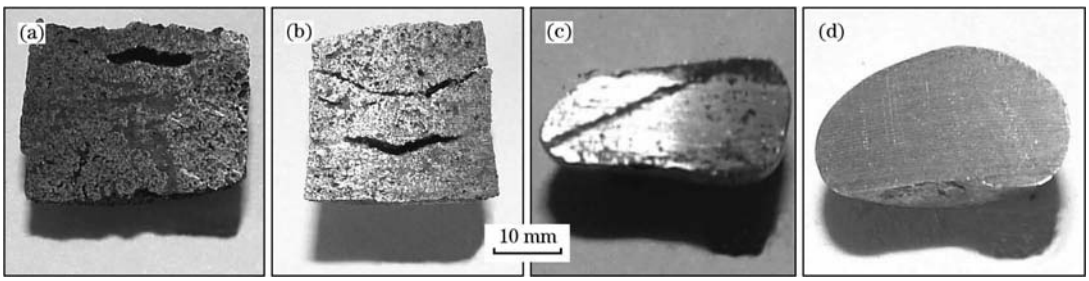

Melting temperature: 1823 K; Na_2CO_3 mixing ratio: 2%.
(a) 1 min; (b) 2 min; (c) 3 min; (d) 4 min.

Fig. 3 Cross-section images of the obtained metal parts at different melting time

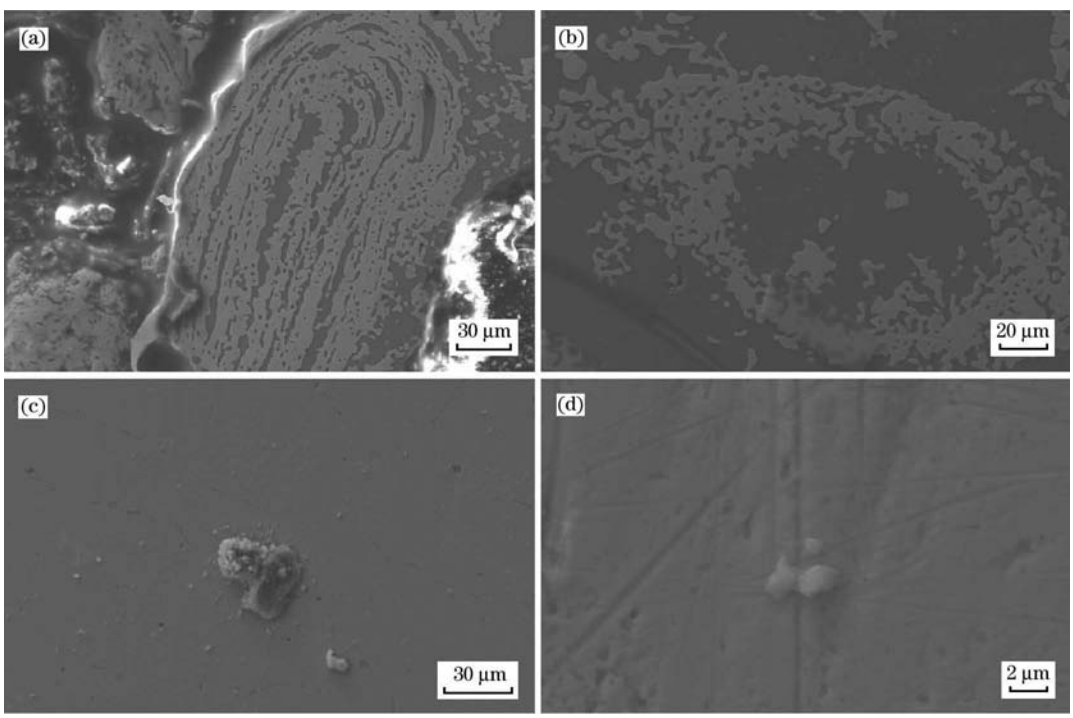

Melting temperature: 1823 K; Na_2CO_3 mixing ratio: 2%.
(a) 1 min; (b) 2 min; (c) 3 min; (d) 4 min.

Fig. 4 SEM images of the metal parts obtained at different melting time

as most solid to liquid transitions had finished, the sample crumbled and a primary metal part was formed with many pores and slag inclusions inside (Fig. 3(c)). Size of typical slag inclusions was more than 30 μm (Fig. 4(c)). When melting time reached 4 min, comparatively big slag inclusions and gas bubbles in hot metal had floated up sufficiently, so the hot metal got purified and it finally changed to an near-sphere shape, size of typical slag inclusions was as small as 2 μm (Fig. 4(d)). The above analysis indicates that good slag/metal separation of the sample needs at least 4 min.

2.2 Phosphorus distribution and iron recovery

2.2.1 *Thermodynamic consideration*

Several theories have been proposed to estimate phosphorus partition ratio between slag and hot metal[9-11]. In the present research, gangues, unreduced iron oxide (wüstite) and additives in the sample formed a very complicated slag system. To take a full consideration of effects of various components on phosphorus partition ratio, the coexistence theory of slag structure[11] was applied. In this theory, phosphorus partition ratio at equilibrium is defined as:

$$L_P = \frac{w_{P_2O_5}}{w_P^2} \tag{2}$$

where, L_P is phosphorus partition ratio; $w_{P_2O_5}$ is P_2O_5 concentration in slag melt, mass%; and w_P is P concentration in metal melt, mass%.

The investigated slag system is considered to be CaO-MgO-MnO-FeO-Al_2O_3-P_2O_5-SiO_2-Na_2O as additive Na_2CO_3 is decomposed to Na_2O and CO_2 at temperature above 1673 K. Structural units of the investigated slag system were selected with a reference to the slag system of CaO-MgO-MnO-FeO-Fe_2O_3-Al_2O_3-P_2O_5-SiO_2[11] and conclusions in Refs. [8, 12]. Ions include Fe^{2+}, Mg^{2+}, Ca^{2+}, Mn^{2+}, Na^+, and O^{2-}, while simple oxides include SiO_2, P_2O_5, Al_2O_3 and complicated compounds include $3FeO \cdot P_2O_5$, $4FeO \cdot P_2O_5$, $2MgO \cdot P_2O_5$, $3MgO \cdot P_2O_5$, $2CaO \cdot P_2O_5$, $3CaO \cdot P_2O_5$, $4CaO \cdot P_2O_5$, $3MnO \cdot P_2O_5$, $3Na_2O \cdot P_2O_5$, $MgO \cdot SiO_2$, $2MgO \cdot SiO_2$, $CaO \cdot SiO_2$, $2CaO \cdot SiO_2$, $3CaO \cdot SiO_2$, $MnO \cdot SiO_2$, $2MnO \cdot SiO_2$, $2FeO \cdot SiO_2$, $Na_2O \cdot SiO_2$, $CaO \cdot MgO \cdot SiO_2$, $3CaO \cdot Al_2O_3$, $12CaO \cdot 7Al_2O_3$, $CaO \cdot MgO \cdot 2SiO_2$, $2CaO \cdot MgO \cdot 2SiO_2$, $3CaO \cdot MgO \cdot 2SiO_2$, $CaO \cdot 6Al_2O_3$, $MgO \cdot Al_2O_3$, $FeO \cdot Al_2O_3$, $3Al_2O_3 \cdot 2SiO_2$, $CaO \cdot Al_2O_3$, $CaO \cdot 2Al_2O_3$, $CaO \cdot Al_2O_3 \cdot 2SiO_2$, $2CaO \cdot Al_2O_3 \cdot SiO_2$.

Thermodynamic data of complicated compounds involving Na_2O is given in Eqs. (3) and (4)[12] and others could be found in Ref. [11].

$$(2Na^+ + O^{2-}) + SiO_2 = Na_2O \cdot SiO_2$$

$$K_{Na_2O \cdot SiO_2} = \exp\left(\frac{134\,055.2 + 40.02T}{RT}\right) \tag{3}$$

$$3(2Na^+ + O^{2-}) + P_2O_5 = 3Na_2O \cdot P_2O_5$$

$$K_{3Na_2O \cdot P_2O_5} = \exp\left(\frac{1\,017\,734 - 257.1T}{RT}\right) \tag{4}$$

Phosphorus partition ratio is then calculated by Eq. (5)

$$\begin{aligned} L_P = 141.94 N_{FeO}^5 \sum n K_0 (1 &+ K_{3FeO \cdot P_2O_5} N_{FeO}^3 + \\ & K_{4FeO \cdot P_2O_5} N_{FeO}^4 + K_{2MgO \cdot P_2O_5} N_{MgO}^2 + \\ & K_{3MgO \cdot P_2O_5} N_{MgO}^3 + K_{2CaO \cdot P_2O_5} N_{CaO}^2 + \\ & K_{3CaO \cdot P_2O_5} N_{CaO}^3 + K_{4CaO \cdot P_2O_5} N_{CaO}^4 + \\ & K_{3MnO \cdot P_2O_5} N_{MnO}^3 + K_{3Na_2O \cdot P_2O_5} N_{Na_2O}^3) \end{aligned} \tag{5}$$

where, K_i is chemical equilibrium constant; $\sum n$ is moles of total units and N_i is mass action concentration represented by mole fraction.

2.2.2 *Effect of Na_2CO_3 additive*

Fig. 5(a) shows that Na_2CO_3 is necessary to retain phosphorus in the slag as w_P is higher than 0.5 mass% in the sample free of Na_2CO_3 and it drops to about 0.3 mass% in the sample with Na_2CO_3 mixing ratio of more than 3%. Thermodynamic calculation indicates that L_P increases with an increase of Na_2CO_3 mixing ratio; however, experiments indicate that maximum L_P appears when Na_2CO_3 mixing ratio is near 3%. The thermodynamic calculations agree well with experimental results when Na_2CO_3 mixing ratio is less than 3%, but serious deviation comes when it is more than 3%. The deviation increas-

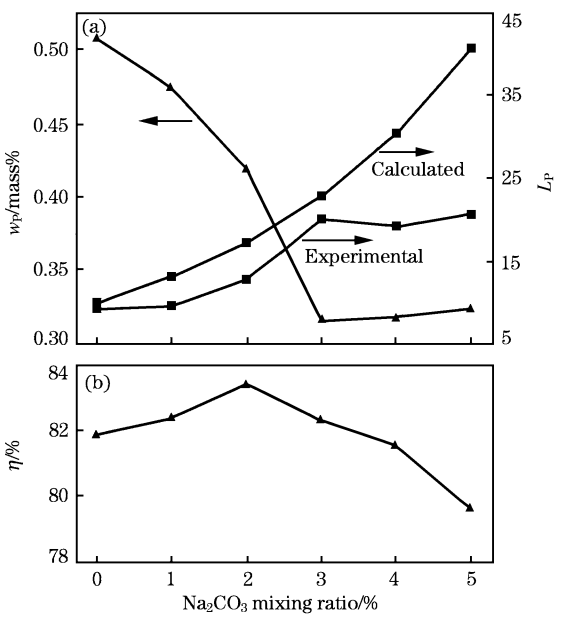

Melting temperature: 1823 K; Melting time: 10 min.
(a) Phosphorus distribution; (b) Iron recovery.

Fig. 5 Effect of Na_2CO_3 mixing ratio on separation results

ing is mainly due to that Na_2O may evaporate at temperature above 1673 K and furthermore the evaporation becomes severe as Na_2CO_3 mixing ratio increases. Na_2CO_3 mixing ratio about 3% is adequate to keep phosphorus in the slag and qualified hot metal for steelmaking could be obtained. From Fig. 5(b), it could be seen that η is 80%—83% when Na_2CO_3 mixing ratio is 0—5%. This indicates that effect of Na_2CO_3 additive is negligible on iron recovery.

2.2.3 Effect of melting time

Fig. 6(a) shows that w_P increases with the increase of melting time when the melting time is 0—20 min, and it is nearly stable when the melting time is more than 20 min; variation of w_P is within 0.04 mass% through the whole melting period. Thermodynamic calculation using the above model indicates that L_P is 26; as the corresponding experimental value is 22—32, it is considered that the model prediction agrees with the experimental measurements. The comparison indicates that phosphorus distribution can be near equilibrium when the melting time reaches 5 min. The above section on slag/metal separation behavior has discovered that the period when the melting time is 0—5 min is mainly for solid-to-liquid transitions; it is thus deduced that L_P can reach equilibrium value as soon as these changes are completed. Fig. 6(b) shows the effect of melting time on iron recovery. It indicates that η undergoes a successive decrease as the melting time extends; however, η still could keep higher than 80% even when the melting time is as long as 30 min.

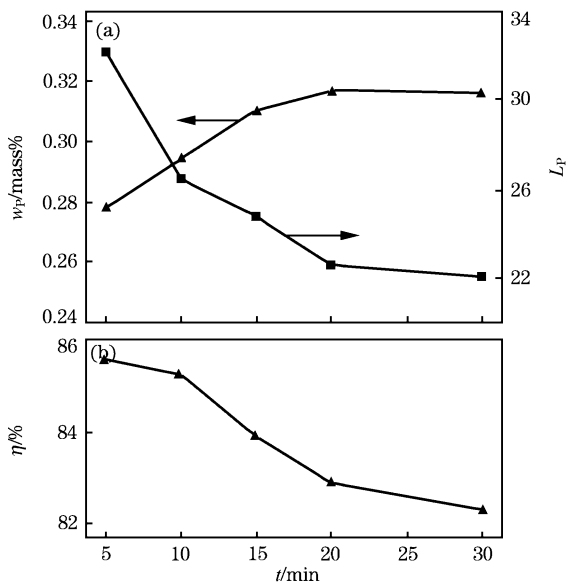

Melting temperature: 1823 K; Na_2CO_3 mixing ratio: 3%.
(a) Phosphorus distribution; (b) Iron recovery.

Fig. 6 Effect of melting time on separation results

SEM images in Figs. 4(a) and 4(b) show that metallic iron layers and gangue layers within the ore particle intimately contact at the initial stage of melting separation, so slag/metal interface area is very large during the separation process and could provide a good kinetic condition for phosphorus transfer. Hence phosphorus distribution can reach equilibrium in a short time.

2.2.4 Effect of melting temperature

Fig. 7(a) shows the effect of melting temperature on phosphorus distribution. Both the calculations and the experimental results indicate that low temperature favors phosphorus remaining in slag. Temperature above 1873 K is not suitable for melting as w_P is higher than 0.4 mass%. As for iron recovery, experimental results are given in Fig. 7(b). Fig. 7(b) shows that η decreases with the increase of melting temperature though its variation is not evident.

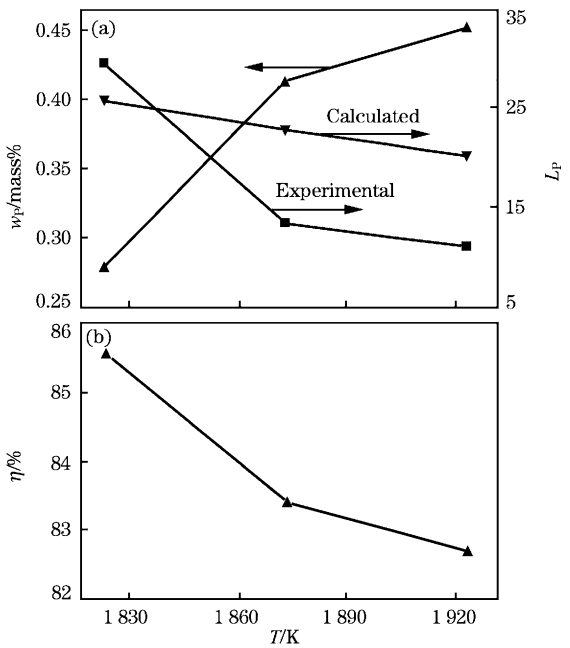

Melting time: 5 min; Na_2CO_3 mixing ratio: 3%.
(a) Phosphorus distribution; (b) Iron recovery.

Fig. 7 Effect of melting temperature on separation results

3 Conclusions

(1) Temperature for slag/metal separation should be more than 1823 K. At that temperature, a good slag/metal separation of the highly reduced ore fines needs at least 4 min.

(2) Phosphorus content of hot metal after separation is mainly determined by the thermodynamic equilibrium. Temperature and Na_2CO_3 mixing ratio are

two key factors. The favorable conditions are temperature of 1823—1873 K and Na_2CO_3 mixing ratio of about 3%.

(3) Temperature, time and Na_2CO_3 mixing ratio do not have significant effect on iron recovery. Iron recovery rate could exceed 80% as long as a good slag/metal separation result is obtained.

References:

[1] J. R. Zhang, L. K. Hu, Y. Y. Liang, H. P. Yang, D. Sun, Chin. Min. J. 16 (2007) 74-76.

[2] L. J. He, F. R. Hu, Min. Metall. 9 (2009) 31-35.

[3] J. Liu, G. Q. Li, C. Y. Zhu. A. C. Wang, J. Mater. Metall. 6 (2007) 173-179.

[4] C. Y. Xu, T. C. Sun, C. Y. Qi, Y. L. Li, X. L. Mo, D. W. Yan, Z. X. Li, B. L. Xin, Trans. Nonferrous Met. Soc. Chin. 22 (2012) 2806-2812.

[5] H. Q. Tang, Z. C. Guo, Z. L. Zhao, J. Iron Steel Res. Int. 17 (2010) No. 9, 1-6.

[6] H. Q. Tang, J. W. Wang, Z. C. Guo, T. Ou, J. Iron Steel Res. Int. 20 (2013) No. 5, 24-29.

[7] T. Morita, M. Fujii, Trans. ISIJ Int. 21 (1981) 732-744.

[8] K. Harashima, M. Matsuo, S. Mizoguchi, Trans. ISIJ 28 (1988) 172-178.

[9] C. Nassaralla, R. J. Fruehan, D. J. Min, Metall. Trans. B 22 (1991) 33-38.

[10] H. B. Zhang, L. Y. Dong, D. F. Chen, F. S. Zhen, C. S. Sun, Chin. J. Process Eng. 9 (2009) 137-141.

[11] J. Zhang, Thermodynamics Calculation of Metallurgy Melt and Solutions, Metallurgical Industry Press, Beijing, 2007.

[12] D. Z. Wang, Dephosphorization in Ironmaking and Steelmaking, Metallurgical Industry Press, Beijing, 1983.